DESIGN AND ANALYSIS OF 8/6 POLE SWITCHED RELUCTANCE MOTOR UNDER TRANSIENT TENURE USING FINITE ELEMENT TECHNIQUE

M. Durairasan[1], S.Sridharan[2], G. Ganesan @ Subramanian[3]

[1,2] *Assistant Professor, University college of Engineering, Thirukkuvalai*
[3] *Assistant Professor, E.G.S. Pillay Engineering College, Nagapattinam*

email: durairasan.m@gmail.com; sridhartvr@gmail.com; ganesan@egspec.org

Abstract: *This paper presents an Electromagnetic and Thermal analysis under transient conditions of a 8/6 pole Switched Reluctance Motor (SRM) using 2D finite element method (FEM). SRM uses reluctance torque which comes from the change of the reluctance of magnetic circuit can be thought of as a type of synchronous motor. However, compared with a regular synchronous, no field winding, slip ring and brushes are used in addition, instead of using a permanent magnet as a rotor. Recently, following the developments of power electronics, the interest in SRM has risen year after year. Electromagnetic & Thermal simulations of SRM are done by using the design software ANSYS. Finite Element Analysis plays a vital role in designing of 8/6pole SRM model which completely eliminates the manual calculations. ANSYS is a complete Finite Element software package. For solving numerical based problems in FEM, ANSYS is a general purpose finite element modeling package for numerically solving a wide variety of engineering problems. Plane 53 is chosen for Electromagnetic analysis and Plane 55 for Thermal analysis of SRM model. The simulation results for various rotor positions are obtained. Most of the analysis are carried out in 6/4 pole SRM but in the proposed method, Electromagnetic & Thermal simulations are obtained under transient conditions for 8/6pole SRM model*

Key words: *SRM, 2D, ANSYS, FEM*

1. INTRODUCTION

Since 1969, a variable reluctance motor has been proposed for variable speed applications. The origin of this motor can be traced back to 1842, but the "reinvention" has been possible due to the advent of inexpensive, high-power switching devices. Even though this machine is a type of synchronous machine, it has certain novel features. It has wound field coils of a dc motor for its stator windings and has no coils or magnets on its rotor.

Both the stator and rotor have salient poles, hence the machine is referred to as a doubly salient machine.

The rotor is aligned whenever diametrically opposite stator poles are excited. SRM is an electrical machine in which the torque developed by means of variable reluctance principle. In this paper, 8/6 pole SRM model is chosen for analysis. Electromagnetic and thermal analysis plays an vital role in designing the SRM model. The simulations are carried out by using 2D finite element method. In FEM, the design is modeled using discrete building blocks called *elements*. The elements have a finite number of unknowns, named *finite elements*. Complete FEM software package used by engineers are ANSYS which is useful for structural analysis, transient analysis, thermal analysis, circuit coupling and Electromagnetic Analysis.

1. DESIGN OF SRM

Using the design software called "ANSYS" , the model of the Switched Reluctance Motor is designed. The design model of 8/6 SRM is as shown in fig. 1. In general, the machines are designed from their output Equations. In SRM, output Mechanical energy can be determined from their 'flux linkage' Vs 'current' characteristics.

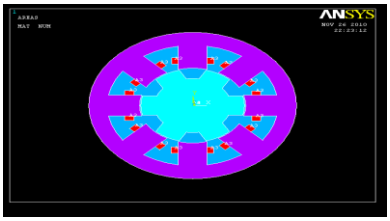

Fig. 1 8/6 pole SRM model

The area enclosed between aligned position and unaligned position curve in the chart denotes output Mechanical energy of the machine for one stroke.

Power developed in SRM is given by

$$P_d = k_c k_d V I m \qquad (1)$$

Where , V and I are peak phase values; k_d = Duty cycle; k_c = Efficiency; m = No. of phases

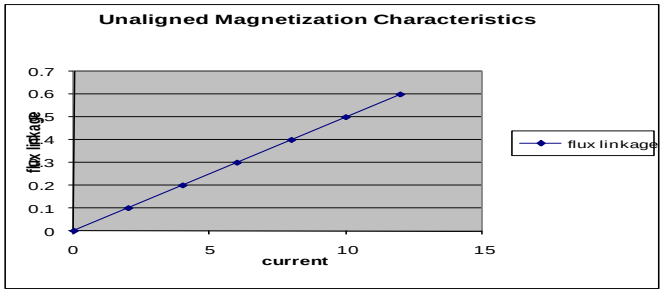

Fig.2 Unaligned characteristics

The aligned and unaligned magnetization chracteristics analysis of SRM shows the mechanical power output of the machine which as shown in fig. 2 and fig.3.

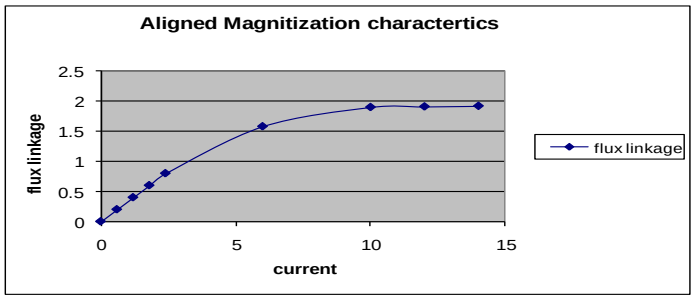

Fig.3 Aligned characteristics

a) Dimensions of an SRM

- Number of stator/rotor poles 8/6
- Power rating : 5KW, 110 turns/phase
- Voltage/current : 220V, 15A
- Speed : 1000 RPM
- Stator diameter outer / inner (45*2) / (37*2)mm
- Rotor diameter outer/ inner (1 6.6*2)/(8.3*2) mm
- Shaft diameter 16.6mm
- Stack length (Lstk) 45mm
- Overall length (Le) 73.6mm
- Air gap 0.5mm

b) Derivation of Output Equation

The output equation relates the bore diameter, length, speed and magnetic and electric loadings to the output of a machine. The output equation for SRM will make its design systematic. Moreover, the experience of the machine designers can be effectively used in the design of these new machines, as they could use the commonality between these and the conventional machines to start with. While the output equation of SRM will be significantly different from that of the conventional machine, the emphasis here is placed on their similarities. The flux linkage and voltage relationship for a flat-topped current I is obtained by neglecting resistive voltage drop as

$$V = \frac{d\lambda}{dt} = \frac{(\lambda_a - \lambda_u)}{\lambda_u} = \frac{(L^s_a - L_u)i}{t} \qquad (2)$$

Where L^S_a is the aligned saturated inductance per phase, L_n is the unaligned inductance per phase, V is the applied voltage and t is the time taken for the

rotor to move from the unaligned to aligned position. That time cab be expressed in terms of the stator pole are and rotor speed as:

$$t = \frac{\beta_s}{\omega_m} \qquad (3)$$

Where β_s is the stator pole are in rad, and ω_m is the rotor speed in rad/s we define.

$$\sigma_s = \frac{L^s_a}{L^\mu_a} \qquad (4)$$

L^μ_a is the aligned but unsaturated inductance, substituting Eqs, the applied voltage becomes :

$$V = \frac{\omega_m}{\beta_s} L^s_a i \left(1 - \frac{1}{\sigma_s \sigma_u}\right) \qquad (5)$$

The power developed then is

$$P_d = k_e k_d V_{im} \qquad (2.5)$$

Where V and i are peak phase values, k_d is the duty cycle defined ,and k_e is the efficiency. The duty cycle can be expressed as :

$$K_d = \frac{\theta_i . q P_r}{360} \qquad (6)$$

Where Φ_1 is the current conduction angle for each rising inductance profile, q is the number of stator poles phases given by P_S /2, P_S is the number of stator poles, and P_r is the number of rotor poles.

$$P_d = K_e K_d \left(\frac{\pi^2}{120}\right)\left(1 - \frac{1}{\sigma_s \sigma_u}\right) BA_s D^2 L N_r \qquad (7)$$

Where N_r is the rotor speed in revolutions per minute(rpm). Can be rearranged to resemble that of the conventional output equation of ac machines and is given by:

$$P_d = K_c K_d K_1 K_2 B A_s D^2 L N \qquad (8)$$

The torque can be obtained from and expressed as :

$$T = k_d k_c k_1 k_2 (BAs) D^2 L \qquad (9)$$

Where

$$K_3 = \frac{\pi}{4} \qquad (10)$$

Thus the torque output are proportional to the product of specific electric and magnetic loadings and bore volume given by ($\pi D^2 L$)/4. k_2 is the only variable dependent on the operating point of the motor and is determined by the stator phase current, magnetic characteristics of the core materials and dimensions. For that matter, the flux linkages vs current for the aligned and unaligned positions are to be estimated for various values of stator current for k_d =1, the power developed is maximum for a given stator current. It is usual to find that the maximum possible duty cycle is less than one.

Furthermore torque and power control are exercised by the duty cycle similar to a chopper-controlled dc motor. The speed is controlled by the frequency of switching of the phases resembling that of a synchronous motor.

c) Material used

Silicon steel is undoubtedly the most important soft magnetic material in use today. It can be mostly used in generators, motors, and transformers. Continued growth in electrical power generation has required development of better steels to decrease wasteful dissipation of energy (as heat) in electrical apparatus. The earliest soft magnetic material was iron, which contained many impurities. Resistivity, which is quite low in iron, increases markedly with the addition of silicon. Higher resistivity lessens the core loss by reducing the eddy current component.

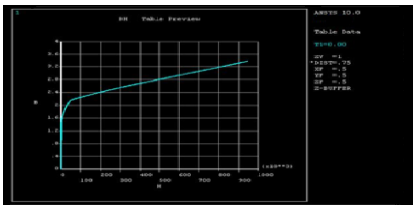

Fig. 4 BH curve of M19 steel

Researchers found that the addition of silicon will lower magnetostriction, increased resistivity, decreased hysteresis loss, increased permeability, and virtually eliminated aging. Relay steels contain 1.25 to 2.5% Si, and are used in direct current applications because of better permeability, lower coercive force, and freedom from aging. Important physical properties of silicon steels include resistivity, saturation induction, magneto-crystalline anisotropy, magnetostriction, and Curie temperature. Relay steels, used widely in relays, armatures, and solenoids. Table 1 shows the BH values of M19 steel which are used for the analysis. As the saturation in the magnetic circuit increases, the losses will also get increased. So the B-H curve analysis of the material is very important in the analysis of the switched reluctance motor because the material property can entirely change the performance of the switched reluctance motor. Also the saturation of the material is found from the B-H curve of the material used.

II. NUMERICAL 2D FINITE ELEMENT ANALYSIS

a) Conductor dimension of SRM in FEA analysis:

In finite element analysis the conductor dimension plays the important role. Fig.5 shows the conductor dimensions of SRM drive. Since we are giving the excitation to the conductor by means of current density ,it is very essential to maintain the correct surface area and volume of the conductor.

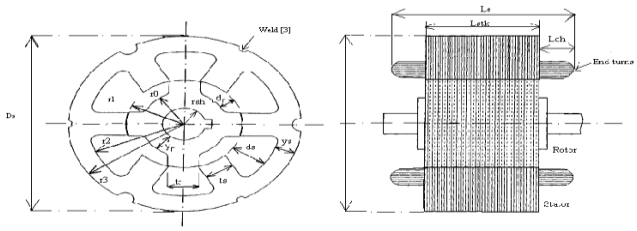

Fig: 5 Dimensions of SRM

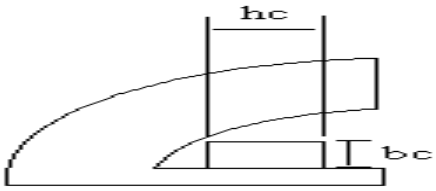

Fig. 6 Conductor Dimensions

Using the volume formula given below the hc and bc values are predicted for the switched reluctance motor.

$$Vol_{cu} = 2.h_c.b_c.L_{stk}.N_s$$

b) Excitation method:

The excitation method for the two dimensional finite element analysis is applying current density as excitation load. The current is given in the form of current density. We know that the current density (J) is equal to the number of turns of the conductor (N) multiplied by the current (I) divided by area of the conductor region (A).it can be mathematically expressed as, J = (NI)/A**.** For our switched reluctance motor dimension the current given is 15 A, the number of turns is 110 turns and the area is 0.000072 mm^2 so we can obtain the J=22916666.6 A/mm^2.

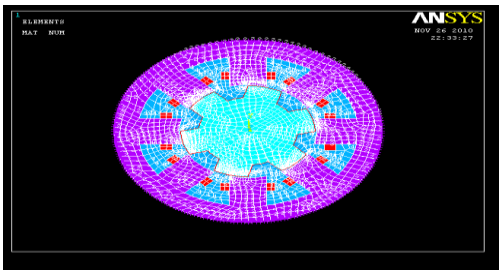

Fig. 7 Excited model of 8/6 SRM

In FEM analysis for the switched reluctance motor we can excite the upper half of the one phase conductor area by (J) and another lower half of the same phase conductor area by (-J).

c) Boundary condition:

We are giving magnetic boundary condition for the switched reluctance motor at the boundary of the stator outer periphery as vector potential AZ = 0(i.e. the magnetic flux will not flow outside that boundary. The following assumptions are made in finding the magnetic field distribution inside the motor using finite element analysis. Magnetic vector potential(A) and current density(j) has only Z-directed Magnetic materials of stator and rotor are isotropic and the magnetization curve is single valued. The outer periphery of the stator can be treated as a zero vector potential line with the magnetic field outside the stator is negligible. End effects are neglected. Then the solution is done to obtain the analysis results. The inductance profile obtained at the operating current indicates that the electromagnetic torque in SRM is a function of variation of excited phase inductance with the rotor position and is expressed mathematically as

$$T = (i^2/2) * dL(\Theta)/d\Theta;\ i = \text{constant} \qquad (11)$$

The average Electromagnetic torque equation is given as,

$$T_{avg} = \frac{1}{n}\sum_{i=1}^{n} T_i \qquad (12)$$

Where, Ti - Instantaneous torque
n - Number of rotor position

III. ELECTROMAGNETIC ANALYSIS

The requirement for finding the performance characteristics of the SRM is to generate the relationships between the flux linkages Vs rotor position as a function of the machine phase currents. This section develops a procedure for analytically deriving the machine characteristics given the motor dimensions and excitation conditions along with the number of turns per phase. Notably, the non linear characteristics of the lamination material are preserved in this method to get a meaningful characterization of the SRM.

In the organization of CAD packages, the system may be regarded as having three identifiable modules as follows in ANSYS.

1.A Pre-processor that enables the user to define the problems geometry and specify boundary condition and excitation sources.

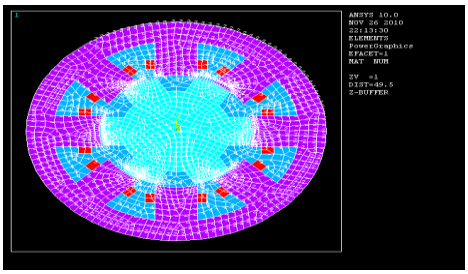

Fig.8 Aligned meshed model of SRM

Mesh generation is conceptually a pre-processing operation and, at this stage, the number of sub- division of primitives and tolerances are set and materials properties are specified. The meshed model of the machine is as shown in fig5& 6.

2. A Solver for constructing the system of algebraic equation, which model the physical situation mathematically, and produces solutions. Solutions are usually given as a set of nodal potentials.

3. A Post-processor that allows the retrieval and analysis of results. At this stage, it is possible to visualize and manipulate the fields and to calculate

important design parameters such as Torque, Inductance and losses.

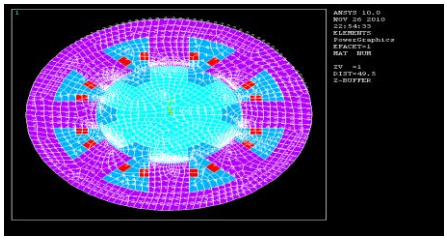

Fig.9 Aligned meshed model of SRM

The area enclosed between the curves 'λ' Vs 'I' for unaligned and aligned positions of the rotor poles gives the maximum work done for one stroke of the motor. The calculation of torque and work done appears to be simple, the data generation for their calculation is a complex process. The data required for this procedure are the flux linkages Vs stator excitation currents for discrete positions of the rotor. The aligned position corresponds to the centre of the stator and rotor poles coinciding, and the unaligned position with the midpoint of the interpolar rotor gap facing the stator pole. It is possible to calculate the flux linkages for the aligned position analytically due to the fact that the leakage flux is negligible in the aligned position. The same is not true for the unaligned position; because the leakage paths are not known a priori, it is not easy to calculate the leakage flux analytically.

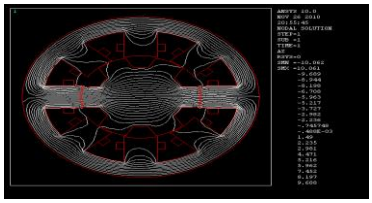

Fig.10 Aligned flux plot of SRM

Finite elements analysis techniques are used to estimate the flux linkages.

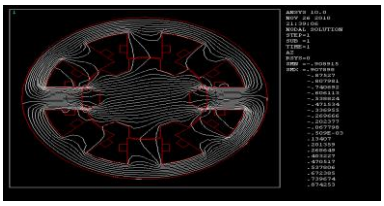

Fig.11 Unaligned flux plot of SRM

The above Fig.7 &8 shows the flux plots under different rotor positions of 8/6 pole SRM respectively. It is clear from the fig.7, that the flux paths in the aligned position are very typical to predict, thus the complexity of the steady state performance evaluation. It is usual to use finite element analysis techniques to map the flux in the unaligned position and for positions in between the aligned and unaligned stator and rotor poles. The flux leakage in the aligned position is practically negligible for the 6/4 SRMs, respectively. Therefore, the analytical calculation of the stator flux linkage at the aligned position is very accurate. The accuracy usually is within 2% of the finite element solution.

a) Flux density evaluation

Consider the complete unaligned position and flux path to illustrate the procedure for evaluating flux densities in various parts of the machine. The flux paths are equi-flux lines. The flux distribution is symmetric with respect to the center line of the excited stator poles.

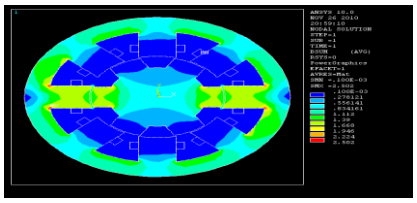

Fig: 12 Flux Density Contour Plot

The flux in each segment of the machine is known and accordingly the flux densities for these segments are evaluated. Let the area of cross section of the flux path in the stator. pole, air gap, rotor back iron, and stator back iron be ASP1., A_g., A_{ry}., and A_{sy} respectively. If the stator flux density is Bsp then the flux in path in the stator is found. A simple magnetic flux density model of the machine representing the vector sum of the flux density is as

shown in the fig. 8. The flux path encloses one quarter of the stator pole are therefore, the area of the cross section is given by

ASP_1 = (1/4) *(Stator pole area) = (1/4) (D/2*βs-L) =(1/8)*(DL)*βs (13)

where 'D' is the inner stator diameter

'βs' is the stator pole arc

'L' is the stator iron stack length.

b) Evaluation of MMF

The mmf for each segment of the flux path is evaluated by finding the magnetic field intensities from the flux densities of the segments using the B-H Curve of the lamination material and average length of the flux path in the segments. The B-H curve analysis of the material is very important in the analysis of the switched reluctance motor because the material property can entirely change the performance of the switched reluctance motor.

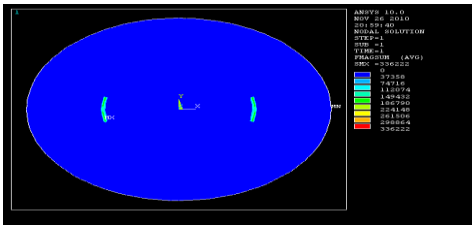

Fig: 13 MMF Contour Plot

Also the saturation of the material is found from the B-H curve of the material used. Usually the mmf error is not attempted in practice due to the large number of iterations; therefore, the mmf error is reduced to a lower tolerance limit. Figure 9 shows the MMF contour plot for the SRM.

IV. THERMAL ANALYSIS

a) Steady-State Thermal Analysis

The ANSYS Multiphysics, ANSYS Mechanical, ANSYS FLOTRAN, and ANSYS Professional products support steady-state thermal analysis. A steady-state thermal analysis calculates the effects of steady thermal loads on a system or component. Engineer/analysts often perform a steady-state analysis before performing a transient thermal analysis, to help establish initial conditions. A steady-state analysis also can be the last step of a transient thermal analysis, performed after all transient effects have diminished.

Steady-state thermal analysis is useful to determine temperatures, thermal gradients, heat flow rates, and heat fluxes in an object that are caused by thermal loads that do not vary over time. Such loads include the following:

Convections, Radiation, Heat flow rates, Heat fluxes (heat flow per unit area), Heat generation rates (heat flow per unit volume), Constant temperature boundaries. A steady-state thermal analysis may be either linear, with constant material properties; or nonlinear, with material properties that depend on temperature. The thermal properties of most material do vary with temperature, so the analysis usually is nonlinear.

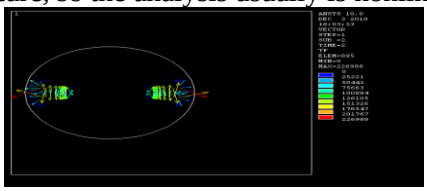

Fig. 14 Thermal flux Plot

Including radiation effects also makes the analysis nonlinear. Thermal plot of SRM model is as shown in fig.10 The procedure for performing a thermal analysis involves three main tasks:
Build the model, Apply loads and obtain the solution & the last one is review the results. Thermal-Electric Analysis in the ANSYS Multiphysics product can

account for the following thermoelectric effects: *Joule heating* - Heating occurs in a conductor carrying an electric current. Joule heat is proportional to the square of the current, and is independent of the current direction. *Seebeck effect* - A voltage (Seebeck EMF) is produced in a thermoelectric material by a temperature difference. The induced voltage is proportional to the temperature difference. The proportionality coefficient is know as the Seebeck coefficient (α) *Peltier effect* - Cooling or heating occurs at the junction of two dissimilar thermoelectric materials when an electric current flows through the junction. Peltier heat is proportional to the current, and changes sign if the current direction is reversed *(b) Thomson effect* - Heat is absorbed or released in a non-uniformly heated thermoelectric material when electric current flows through it.Thomson heat is proportional to the current, and changes sign if the current direction is reversed. Nodal temperature curve of SRM model is shown in fig.11

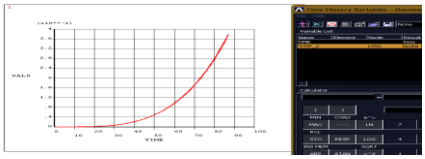

Fig. 15 Nodal temperature curve at Transient conditions

CONCLUSION

This paper has reported the Electromagnetic & Thermal analysis under transient conditions of a 8/6 pole SRM model using two dimensional Finite element methods. Simulated results at various rotor positions such as aligned, unaligned & intermediate positions are obtained for electromagnetic and thermal analysis. Existing methods are replaced with 8/6 pole SRM model. Future work, circuit and FEM domains are coupled and simulated.

REFERENCES

[1] T. J. E. Miller, Ed., Electronic Control of Switched Reluctance Motors. ser. Newnes Power Engineering Series. Oxford, U.K.: Newnes, 2001.

[2] Switched Reluctance Motors and Their Control. Lebanon, OH: Magna Physics/Oxford Univ. Press, 1993.

[3] R. Furmanek, A. French, and G. E. Horst, "Horizontal axis washers," Appliance Manufacturer, pp. 52–53, Mar. 1997.

[4] K. McLaughlin, "Torque ripple control in a practical application," in Electronic Control of Switched Reluctance Motors. ser. Newnes Power Engineering Series, T. J. E. Miller, Ed. Oxford, U.K.: Newnes, 2001, ch. 8.

[5] W. Pengov and R.L. Weinberg, "Designing for low noise," in Electronic Control of Switched Reluctance Motors. ser. Newnes Power Engineering Series, T. J. E. Miller, Ed. Oxford, U.K.: Newnes, 2001, ch. 4.

[6] J. M. Stephenson and J. Corda, "Computation of torque and current in doubly-salient reluctance motors from nonlinear magnetization data," Proc. Inst. Elect. Eng., vol. 126, no. 5, pp. 393–396, 1979.

[7] T. J. E. Miller and M. McGilp, "Nonlinear theory of the switched reluctance motor for rapid computer-aided design," Proc. Inst. Elect. Eng., pt. B, vol. 137, no. 6, pp. 337–347, Nov. 1990.

[8] J. Corda and J. M. Stephenson, "Analytical estimation of the minimum and maximum inductances of a double-salient motor," in Proc. Leeds Int. Conf. Stepping Motors and Systems, Leeds, U.K., Sept. 1979, pp. 50–59.

[9] A. M. Michaelides and C. Pollock, "The effect of end core flux on the performance of the switched reluctance motor," Proc. IEE—Elect. Power Applicat., vol. 141, no. 6, pp. 308–316, Nov. 1994.

[10] A. B. J. Reece and T. W. Preston, Finite Element Methods in Electrical Power Engineering. London, U.K.: Oxford Univ. Press, 2000.

[11] T. J. E. Miller and M. McGilp, PC-SRD User's Manual, Version 7.0. Glasgow, U.K.: SPEED Laboratory, Univ. Glasgow, 1999. MILLER: OPTIMAL DESIGN OF SWITCHED RELUCTANCE MOTORS 27

[12] T. J. E. Miller, M. Glinka, C. Cossar, G. Gallegos-Lopez, D. Ionel, and M. Olaru, "Ultra-fast model of the switched reluctance motor," in Conf. Rec. IEEE-IAS Annu. Meeting, St. Louis, MO, Oct. 1998, pp. 319–326.

[13] P. C. Kjaer, J. J. Gribble, and T. J. E. Miller, "High grade control of switched reluctance machines," IEEE Trans. Ind. Applicat., vol. 33, pp. 1585–1593, Nov./Dec. 1997.

[14] J. W. Finch, M. R. Harris, A. Musoke, and H. M. B. Metwally, "Variablespeed drives using multi-tooth per pole switched reluctance motors," in Proc. 13th Incremental Motion Controls Symp., Univ. Illinois, UrbanaChampaign, IL, 1984, pp. 293–302.

[15] K. Konecny, "Analysis of variable reluctance motor parameters through magnetic field simulations," in Proc. Motor-Con, 1981, p. 2A.

[16] R. S. Colby, F. Mottier, and T. J. E. Miller, "Vibration modes and acoustic noise in a 4-phase switched reluctance motor," IEEE Trans. Ind. Applicat., vol. 32, pp. 1357–1364, Nov./Dec. 1996

[17] F. S. Soares and P. J. Costa Branco, "Simulation of a 6/4 switched reluctance motor based on Matlab/Simulink environment," IEEE Transactions on Aerospace and Elecfronic Systems, Vol. 37, No. 3, July 2001, pp989-1009.

[18] Y. Xu and D.A. Torrey, "Study of the mutually coupled switched reluctance machine using the finite element-circuit coupled method," IEEE Proc-Electr. Power Appl., Vol. 149, No. 2, March 2002, pp81-86.

[19] W. Wu, J. B. Dunlop, S. J. Collocott and B. A. Kalati, "Design optimization of a switched reluctance motor by electromagnetic and thermal finite element analysis," IEEE Transactions on Magnetics, in press Digests of NTERMAGZOO3, Boston, USA, March 30 - April 3, 2003.

[20] N. K. Sheth and K. R. Rajagopal: Estimation of Core Loss in A Switched \ Reluctance Motor Based On Actual Flux Variations, IEEE Paper, 2006

[21] M. Balaji and V. Kamaraj: Evolutionary Computation Based Multi-Objective Pole Shape Optimization of Switched Reluctance Machine, Science Direct, Electrical Power and Energy System43 2012 (63-69)

[22] N. K. Sheth and K. R. Rajagopal: Computer Aided Design of Multi-Phase Switched Reluctance Motor, Journal of Applied Physics 97, 10Q512, May 2005